J. Ind. Geophys. Union, 28(6) (2024), 417-429

A PGA amplification study for Varanasi city (India): Implications for seismic hazard assessment

Anurag Tiwari[1,3], Naresh Rana[2*] and G P Singh[3]
[1]National Center for Seismology, Ministry of Earth Sciences, New Delhi-110003, India
[2]Department of Geology, University of Delhi, Delhi-110007, India
[3]Department of Geophysics, Banaras Hindu University, Varanasi-221005, India
*Corresponding author: nrana@geology.du.ac.in

ABSTRACT

The Indo-Gangetic Plain is one of the most densely populated regions of the world, and the seismo-tectonics of the Himalaya has a profound impact on the seismic hazards on this area. We analysed various seismic and lithological parameters of one of the oldest and most densely populated cities of the Indo-Gangetic Plain, called Varanasi, to assess the seismic risk for the city. This study revealed that the surface geology of this region has a considerable impact on the Peak Ground Acceleration (PGA), which determines the degree of damage in any area after an earthquake. The various factors, such as the population density, thickness of sediment, and building structure pattern of the city, make it highly vulnerable to seismic hazards. In view of this, we have used multiple data sets to assess the seismic amplification for the city. Our results suggest that the surface geology of the area may amplify the signal from 1.7 to 3.2 times in the study area. Thus, the seismic hazard of the area is higher than the expected hazard for seismic zone III.

Keywords: Indo-Gangetic Plain; Peak Ground Acceleration (PGA) amplification, Vs30; Varanasi city; Seismic risk.

INTRODUCTION

Earthquakes are often natural, unavoidable phenomena that are largely unpredictable, especially in terms of time. The knowledge of active faults has constrained the spatial limit of the probable source zone, and their proximity to the area of interest has been extensively employed as a key factor in seismic hazard assessment (Khattri et al., 1984). In general, the amplitude of the seismic wave attenuates with distance, and as a result, the seismic hazard also decreases (Stein and Wysession, 2003). However, recent studies have shown that the earthquake distance alone is not a sufficient criterion for seismic hazard assessment (Celebi et al., 1987; Mohamad et al. 2013; Akkar et al. 2014; Panjamani et al. 2018), and the key elements responsible for damage are site amplification and secondary hazards, such as liquefaction (Idriss and Boulanger, 2008). Furthermore, earthquake risk is affected by construction quality, social awareness, and the population density of the area. Given this, characterization of the local geology in terms of seismic parameters (PGA amplification factor, predominant frequency, and V_s30) response at the site, may play a critical role in assessing seismic risk for densely populated cities. Unfortunately, the Indo-Gangetic Plain, which is India's most densely populated region, is located immediately south of the active Himalayan Frontal Thrust and is prone to earthquakes hazards (Hough and Bilham, 2008; Bajaj and Anbazhagan, 2019). The historical data of the area also shows substantial damage during past Himalayan earthquakes (Ambraseys, 2000). According to Bilham (2009), an earthquake of magnitude ~ 8 in the nearby source region, could claim the lives of 0.3 million people in this region. Furthermore, the building construction practices of the area have been relatively poor (Raghucharan et al., 2021), which may enhance the risk to life and property many folds. The area has been categorized within seismic hazards zone III of India, which has the potential to experience a PGA up to 0.2g (BIS, 2002). However, the thick sedimentary overburden may amplify the seismic wave by site amplification and increase the risk (Hunter et al., 2002; Denolle et al., 2014). An analysis of the site-amplification characteristics of this region could assist in re-evaluating the seismic risk of the area and enhancing the awareness about the potential risk among the general public and decision makers. In addition, the precise estimation of ground motion may help in taking cost-effective mitigation measures and appropriate land use planning (Bommer et al., 2015).

Earthquake micro-zonation attempts to account for changes in sediment overburden, heterogeneity, and soil liquefaction along with many seismotectonic elements in order to determine seismic wave site-amplification for risk reduction (Nath and Thingbaijan, 2009). While several methods have been used to model the site-amplification of seismic waves, one of the most crucial approaches is to use the average shear wave velocity of the upper 30 meters (Vs30) of the soil column (Choi and Stewart, 2005; Kanli et al., 2006). The Vs30 is directly related to soil stiffness and can be determined by geotechnical procedures such as the standard penetration test (STP), which are often carried out for engineering constructions (Kanli et al., 2006). Attempts have been made to calculate the Vs30 using the MASW for Varanasi city earlier (Singh et al., 2020). In this continuity, this study offers preliminary estimations of PGA amplification using the most cost-effective techniques. The

PGA amplification is computed from existing geotechnical data of Varanasi city, situated in the Indo-Gangetic Plain.

STUDY AREA

Local geology and seismotectonics

Varanasi (Figure 1) is one of the oldest and most densely inhabited cities in India, lying in the vast northern alluvial plain of the Ganga River, which has extensively shaped the geomorphology of the area (Figure 2). The local geology of the Varanasi is constituted by the a thick (>200m) Quaternary alluvium deposited by the Ganga River (Shukla et al., 2012). An analysis of the bore hole data shows that the grain size of the upper sediment layers varies from clay to gravely sand, expressing the braided and freely migrating channel facies (Shukla and Raju, 2008). This extensive accommodation space has been provided due to the downward flexure of the lithosphere as a result of tectonic compression, where the sediments have been brought in from the Himalaya as well as from the cratonic part of India (Shukla et al., 2012). The basement of the Indo Gangetic Plain is made up of very unevenly metamorphosed Precambrian rocks in the form of trough and ridges, which also control the thickness of the overlying Quaternary alluvium.

As an ancient city, many of the buildings in the city are either very old and damaged or have specific structural weaknesses, making them highly vulnerable to earthquake hazards (Jha and Bajwa, 2023). The presence of a number of geological structures, such as the Faizabad Ridge, Allahabad Fault, Azamgarh Fault, Devoria Fault, Patna Fault, Siwan Fault, and, most importantly, the Himalayan Frontal Thrust, is a matter for concern due to their ability to generate earthquakes or reactivate during large Himalayan earthquakes (Figure 1a) (Sahu and Saha, 2014). The Himalayan Frontal Thrust is the surface expression of the Main Himalayan Thrust, which is the principal decollement facilitating the northward movement of Indian plates that often expressed in the form of large earthquakes (Seeber and Armbruster, 1981). All of the great earthquakes in the Himalaya have been caused by slip along the Main Himalayan Thrust, which often ruptures the Himalayan Frontal Thrust (Bilham, 2019).

The river morphology and lineament study of the area has found evidence of neotectonics (Singh et al., 1996). Based on the chronology of the sediments around Varanasi, Shukla et al., (2012) have demonstrated that the area has undergone a significant tectonic uplift along a fault around 40 ka and 7 ka. They have suggested that currently the area is undergoing extensional tectonics, and the river course around Varanasi is also controlled by a gravity fault. In addition, some evidence of tectonic activity is also reported from the peripheral bulge in the south of Varanasi (Agarwal et al., 2002). These ideas rely on more theoretical surficial geomorphological aspects and lack in-depth geological and geophysical evidence of active faulting. Nevertheless, the extension of the active tectonics in the Indo-Gangetic Plain cannot be denied and needs to be reassessed in view of the seismic risk of the area.

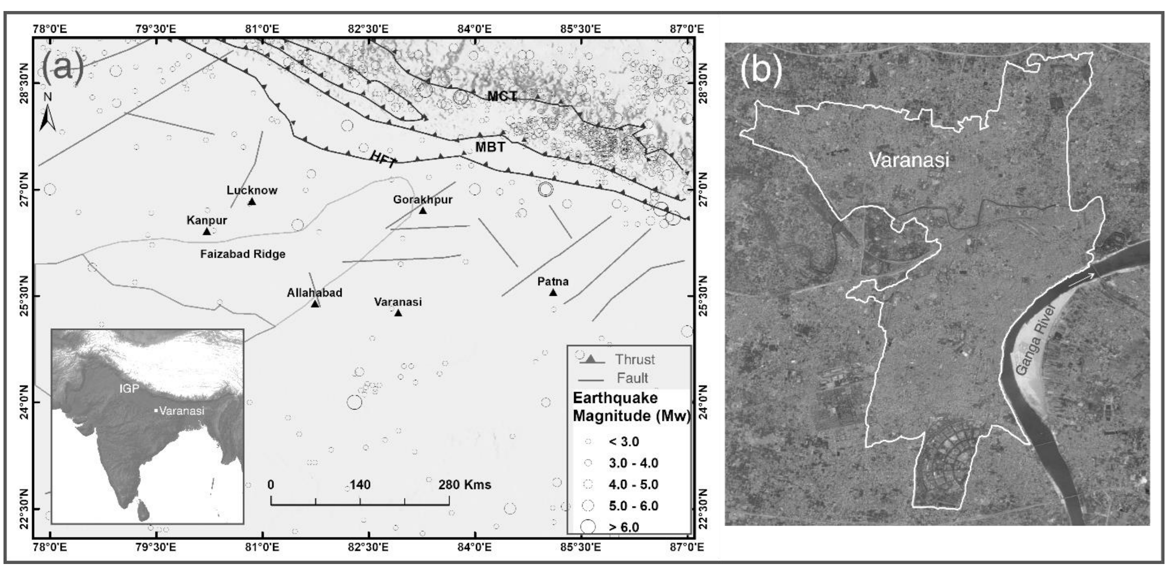

Figure 1. Study area. **(a)** Location of the study area and seismo-tectonics of the region. **(b)** Google Earth satellite image of Varanasi city and the Ganga river. Seismic data plotted according to the NCS website https://riseq.seismo.gov.in/riseq/earthquake for the period from 1900 to 2022. Tectonic boundaries are adapted from GSI (Bhookosh-GSI.gov.in). HFT- Himalayan Frontal Thrust; MBT- Main Boundary Thrust; MCT-Main Central Thrust; IGP- Indo Gangetic Plain.

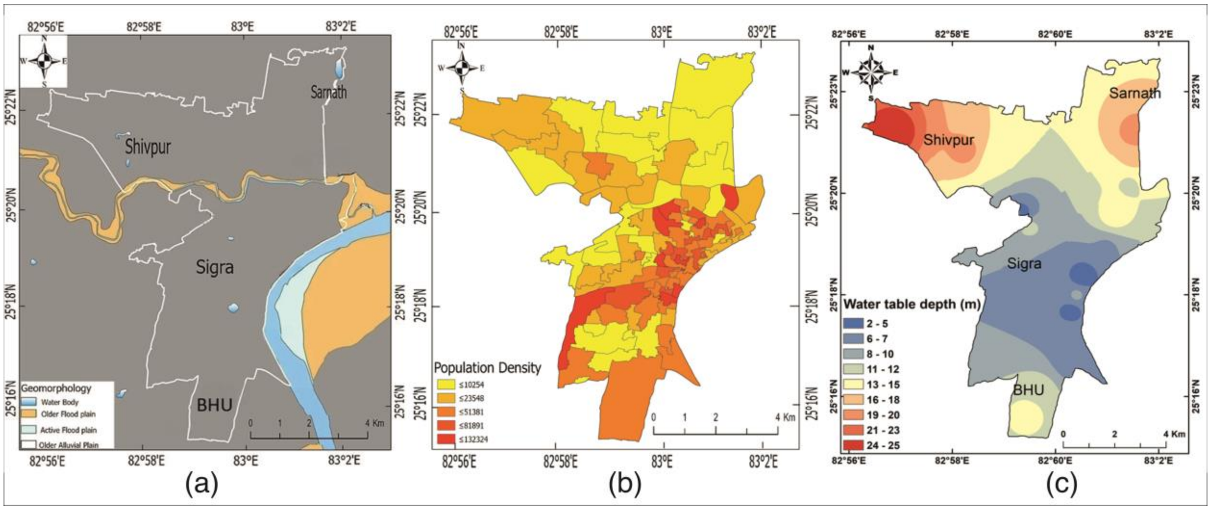

Figure 2. Varanasi city. **(a**) Surface geomorphology, **(b**) Population density and **(c)** Groundwater table.

Table 1. Population growth of the Varanasi city (VDA, 2022).

S No	Year	Population	Population growth	Decadal population growth (%)
1	1931	2,07,650	--	--
2	1941	2,66,002	58352	28
3	1951	3,55,771	89769	34
4	1961	4,89,864	134093	38
5	1971	6,17,934	128070	26
6	1981	7,73,865	155931	25
7	1991	10,00,747	226882	29
8	2001	11,70,897	170150	17
9	2011	15,40,000	369103	32
10	2021	25,71,256	10,31,256	40
11	2031	31,44,646	5,73,390	18

Population and buildings

Varanasi has a dynamic mixture of urban and rural settings, with urbanized zones clustered around the city center and along the riverbanks. The population growth rate of the city has remained significantly increased over successive decades, notwithstanding a recent drop. This demographic boom is being driven by a combination of factors such as natural population growth, migration from adjacent rural areas and other parts of the country, and the increasing rate of urbanization (VDA, 2022). This increased population expansion has placed tremendous demand on the infrastructure and resources of the city, resulting in difficulties ranging from housing to transportation provisions and environmental sustainability (Rana, 2018). All these conditions forced people to reside in the vulnerable buildings. The majority of buildings in the area are old, with families residing in them for three to nine generations. For example, the Chausatti Ghat (area) of the city, is home to the oldest buildings of the city (average 200 to 300 years old), with some of them exceeding five hundred years in age (Bakker, 1996). Many buildings in Varanasi are in a state of disrepair, and individuals from many other states of India are living in these highly vulnerable structures as tenants. The owners, who reside elsewhere, rarely visit Varanasi and have not taken any action to maintain the buildings. Consequently, the tenants live in precarious conditions without proper upkeep (Figure 3).

The projected population for the years 2021 and 2031 is estimated using geometric, arithmetic, and parabolic methods, considering the urbanization plan outlined in the Varanasi Development Authority Master Plan 2031 (VDA, 2022). Varanasi has experienced significant population growth over the years, as evidenced by census data.

Figure 3. Building typology of the Varanasi city (Uttar Pradesh, India)

According to the census report (Table 1), the population of Varanasi city has steadily increased from 2,07,650 in 1931 to 25,71,256 in 2021, representing a remarkable growth of over 1.2 million inhabitants. The decadal population growth rate has fluctuated over time, with peaks observed in the 1950s, 1960s, and 2020s, reaching as high as 40% during certain decades (VDA, 2022). This rapid population expansion, coupled with urbanization and migration trends, has placed immense pressure on the city's infrastructure and resources

Water table

Due to thick alluvium and proximity to Ganga River, the region has abundant groundwater potential. A variety of factors influence the water table dynamics of the city, including precipitation patterns, fluctuating river levels, and groundwater exploitation. The water table depth is noticeably non-uniform across the city, varying from a few meters to 20 meters. In general, the eastern parts, near the Ganga River, have a higher water table than the western sectors. According to the Gautam (2012), an average water table depth of roughly 6.5 meters has been observed for the area. This depth, however, reveals considerable changes over short distances, which are intimately influenced by localized geology, hydrogeology, and land use patterns (Figure 2c).

METHODOLOGY

Peak ground acceleration (PGA) modeling

A computer program called DYNEQ (Yoshida and Suetomi, 1996) was used to conduct a nonlinear site response analysis for the Varanasi city. The investigation focused on the dynamic response of flat ground using the Equivalent linear approach. The DYNEQ program utilized a 1-D nonlinear site response analysis approach to evaluate the vertical transmission of horizontal shear waves in thick soil/sediment layers. The site response was evaluated based on the amplification factor for PGA.

The input acceleration time history was generated using the peak PGA and 5% damped Pseudo-Spectral Acceleration (PSA) values for earthquakes of 2% and 10% probability of exceedance in 50 years modelled by Nath et al. (2019) and Nath (2017) representing both a 475-years and a 2475-years return period scenario. According to them, the PGA at 2% probability of exceedance is approximately double than 10 % probability of exceedance. Specifically, the PGA values from the analysis were utilized for both the 2% and 10% probability of occurrence representing the maximum considered earthquake scenario (MCE) and design basis earthquake scenario (DBE) respectively. PGA at the rock level varies from 0.082g to 0.117g for a scenario of 10 % probability of exceedance (DBE) from 0.174g to 0.194g for a scenario of 2% probability of exceedance (MCE) (Nath, 2017, Nath et al., 2019). These PGA and PSA values were used as input parameters to obtain surface PGA for the area using the computer program (Yoshida and Suetomi, 1996). The program uses the pertinent attributes of soil layers such as groundwater condition, thickness, density, cohesion coefficient, angle of friction, layer velocity, shear wave velocity, and input waveform file.

To generate earthquake waveforms, the process begins by reading spectral parameters (period T and spectral acceleration Sa) at a reference points. Using these parameters, spectral parameters are generated at another location where earthquake records are not available but PGA is known, considering the proximity between the two points. Sa values are normalized with respect to period T and then converted into frequencies (F) in ascending order using the formula F=1/T, representing the spectral characteristics. Subsequently, a response file is generated with input parameters including damping value, total duration, and the computable rise and fall times. This process results in the creation of an acceleration time series file containing 8192 data points with a time increment of 0.005 seconds. The output file is then converted into an eight-column waveform format for further analysis, serving as the input waveform file. This method ensures the generation of accurate earthquake waveforms for seismic analysis.

These inputs are commonly employed in calculating the transfer function of soil strata, which is an influential ratio between output (surface) and input (bedrock) ground motions and are used here to derive the amplification factor. The different soil attributes were obtained from different data sources. The geotechnical data (available for 19 sites), provides the various attributes of soil such as N value, water level depth, and grain size (RITES, 2016). The shear wave velocities were obtained from the published MASW data (Singh et al., 2020). Based on the available data, we used empirical relations to determine shear wave velocity for the 29 locations in the city. The details of the locations and results are given in Table 2. The shear wave velocities were used to determine the engineering bedrock depths for the area (Anbazhagan and Sitaram, 2009). Bedrock Depth is mapped for the shear wave velocity of 760 m/s (Anbazhagan and Sitaram, 2009). The data was used for extrapolation and interpolation done for the study region with the inverse distance weighted technique to depict the results for the whole study region.

Determination of PGA amplification factors

The PGA (Peak Ground Acceleration) amplification factor measures the increase in ground motion from the bedrock to the soil surface. It is calculated as the ratio of the PGA at the soil surface to the PGA at the bedrock (Bajaj and Anbazhagan, 2020). This ratio provides insight into how the presence of soil layers affects the intensity of seismic motion at the surface compared to the bedrock.

Vs30 modeling

The Vs30 value represents the average shear-wave velocity in the top 30 meters of a soil column. It is a key factor that determines the ground motion amplification and duration of earthquake shaking (Borcherdt, 1970, 1994; Kuo et al., 2012). The Vs30 value can be estimated using various methods, including empirical, theoretical, and geophysical methods to estimate the site classes, which can be used to derive the strong motion prediction equation (Boore, 2003).

A frequently employed approach to calculate Vs30 is to correlate it with the N value, which is a measure of the soil stiffness obtained from the SPT. The correlation between Vs30 and N value varies depending on the local geology and soil conditions.

Several empirical equations are available in the literature that relate Vs30 with the N value. Singh et al. (2020) used field N values to calculate the depth-wise shear wave velocity with the relations using N value and shear wave velocity (Vs) for the Varanasi region. They obtained the following correlations:

$$Vs = 70{:}05\ N^{0.49} \quad \ldots\ldots(1)$$

(for all soils)

$$Vs = 74{:}80\ N^{0{:}47} \quad \ldots\ldots(2)$$

(for clayey soil)

Where, Vs is the shear wave velocity in m/s and N represents the 'N-value' of STP. Using these relations, we obtained the Vs at every 3 m up to 30-meter depth. The Vs30 is evaluated with the generalized relation:

$$Vs30 = \frac{\Sigma hi}{\Sigma(hi/Vsi)} \quad \ldots\ldots(3)$$

Where, hi = Thickness of Layer in m; Vsi = Shear wave velocity of layer in m/s.

Based on the dynamic soil properties, a dynamic soil model was developed for the sites. This model considers the effect of soil layers and their thicknesses, soil stratigraphy, shear wave velocity, and other site-specific factors. Using the dynamic soil model, the ground motions at the site were analyzed for the DBE and MCE scenario. This analysis considers the frequency content and amplification of the ground motions due to the soil profile.

RESULTS AND DISCUSSION

PGA amplification

The seismic response of a site can vary significantly depending on local soil conditions and the intensity of ground motion. As illustrated in Figure 4, the acceleration time series at the rock level (green spectrum) undergoes notable amplification when propagating to the surface level (magenta lines). This amplification is demonstrated for two different hazard levels: (a) 10% probability of exceedance and (b) 2% probability of exceedance in 50 years. The comparison between these two scenarios highlights how the degree of amplification can change with the severity of the seismic event, emphasizing the importance of considering site-specific conditions in seismic design and risk assessment. Figure 5 represents how this change occurs from bedrock to surface.

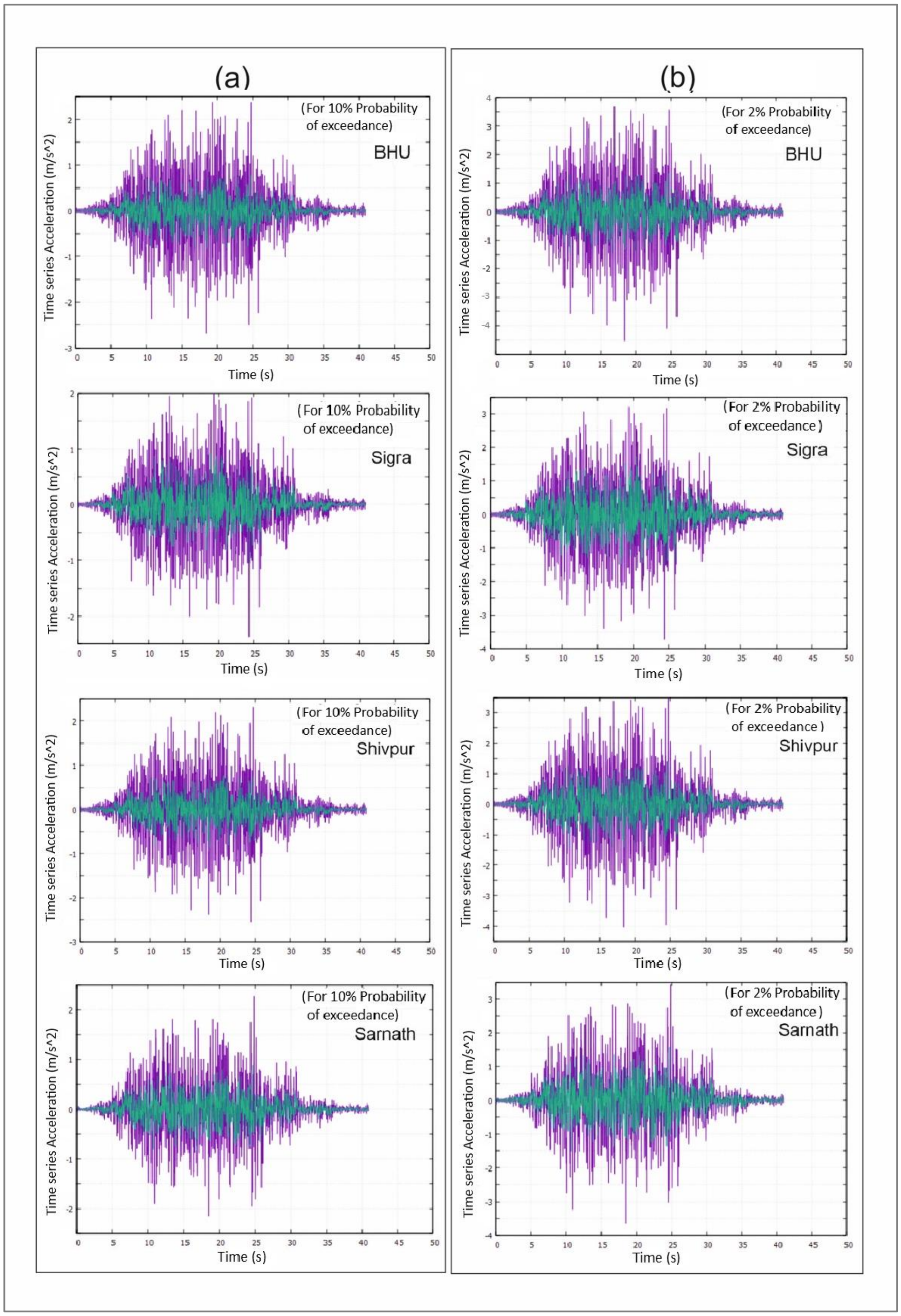

Figure 4. Acceleration time series with 5% damping at rock level shown via green spectrum while amplified acceleration time series at surface level shown by magenta lines for **(a)** 10% probability of exceedance and **(b)** 2% probability of exceedance in 50 years.

The peak ground acceleration (PGA) is a key parameter in earthquake hazard assessment, representing the maximum acceleration experienced by the ground during an earthquake (Parihar and Anbazhagan, 2020; Puri and Jain, 2020). The PGA values are essential for seismic zoning and building code development, which help in delineating the areas of high seismic risk and guiding construction practices accordingly. The calculated surface-level PGA shown in Figure 6 spans from 0.171g to 0.269g for the DBE scenario (i.e., 10% probability of exceedance in 50 years) and 0.280g to 0.454g for the MCE scenario (i.e., 2% probability of exceedance). Figure 7 shows that the PGA amplification factor varies from 1.7 to 3.2 times over the region of Varanasi for both DBE and MCE scenarios. This spectrum of values reflects the substantial variation in ground motion contingent on the seismic scenario in focus. The obtained PGA amplification values correspond to intensified ground motion, thereby augmenting the potential for heightened structural damage to buildings and other infrastructure (Cornell, 1968). According to Nath et al. (2019), the PGA values at the rock level below Varanasi City, range from 0.146-0.172 g, which corresponds to macroseismic zone III. However, due to the site-amplification, the PGA values at the surface in Varanasi are expected to be much higher (e.g. Singh et al., 2023), implying a higher than expected risk for the city.

In Varanasi city, the building pattern typically consists of a mix of traditional low-rise structures, mid-rise buildings, and some recent high-rise developments. Traditional buildings often have one or two stories and are constructed using materials like brick, wood, and mud, which may offer limited resistance to seismic forces (Figure 3). Mid-rise buildings typically range from three to six stories and may incorporate modern engineering techniques, but their vulnerability can vary depending on construction quality and adherence to seismic codes. High-rise buildings, usually above six stories, are relatively less common but can be found in certain areas like Sigra, Lanka, Mahmoorganj, and Bhelupura, particularly in commercial or densely populated zones. The population density in these areas is relatively high due to socioeconomic reasons. In terms of vulnerability, buildings with shorter natural periods of vibration, such as low-rise and mid-rise structures, are generally more susceptible to damage during earthquakes (USGS, 2024). These buildings resonate at frequencies closer to the predominant frequencies of seismic waves, resulting in increased structural response. Additionally, structures with inadequate lateral resistance systems or poor construction quality are at higher risk.

Vertical variation of PGA

The present study examined the vertical variation of PGA values for two different seismic risk scenarios. First, is PGA variation from rock level to surface for 2% probability of exceedance in 50 years representing Figure 5a and second is represented in Figure 5b for 10% probability of exceedance in 50 years.

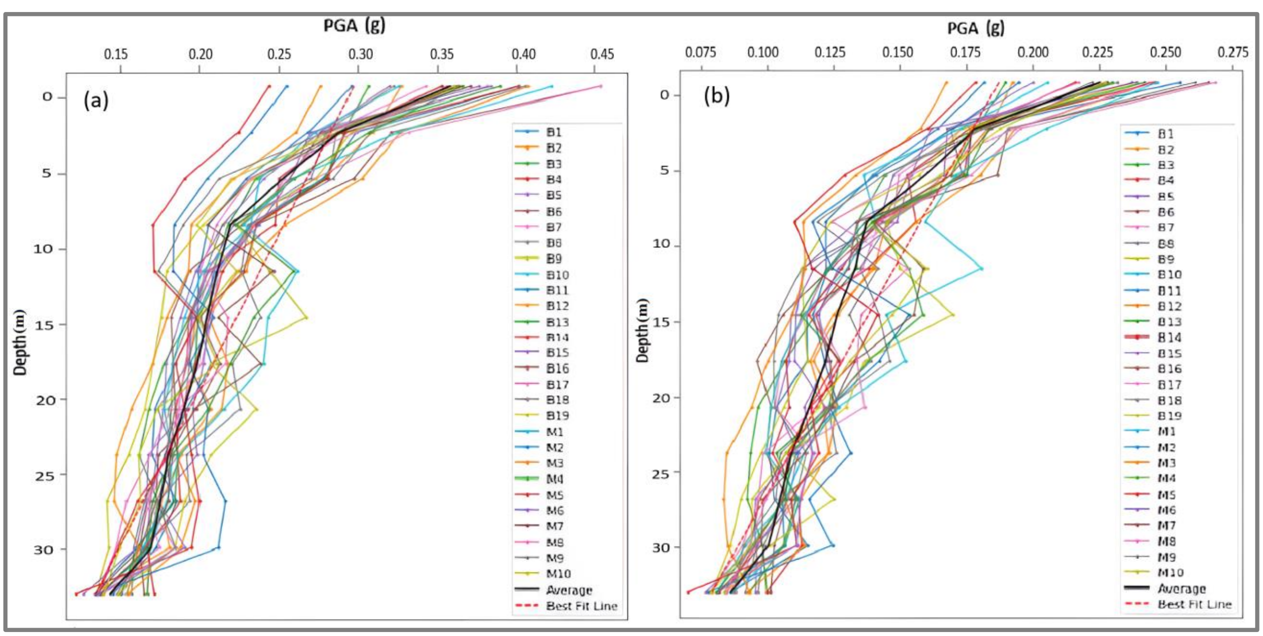

Figure 5. **(a)** vertical variation of PGA (g) for 2 % probability of exceedance in 50 years. **(b)** vertical variation of PGA(g) for 10 % probability of exceedance in 50 years.

The findings indicate a trend where the PGA values decrease from the rock level towards the surface. This attenuation of seismic intensity with decreasing depth has been quantified through linear regression analysis. For the DBE scenario, the relationship between PGA and depth (d) is represented by the equation,

$$PGA = -0.0032\, d + 0.1898 \quad (4)$$

$$R^2 = 0.8452 \quad (5)$$

with an R^2 value of 0.8452, indicating a strong correlation. Similarly, for the MCE scenario, the deduced relationship is given by

$$PGA = -0.0048\, d + 0.3021 \quad (6)$$

$$R^2 = 0.8202 \quad (7)$$

These equations suggest that as depth decreases, the PGA values increases, highlighting a significant dependency of seismic ground motion on depth. The high R^2 values reflect a reliable fit of the linear models to the observed data, demonstrating the predictive capability of these relationships for assessing seismic hazards at varying depths.

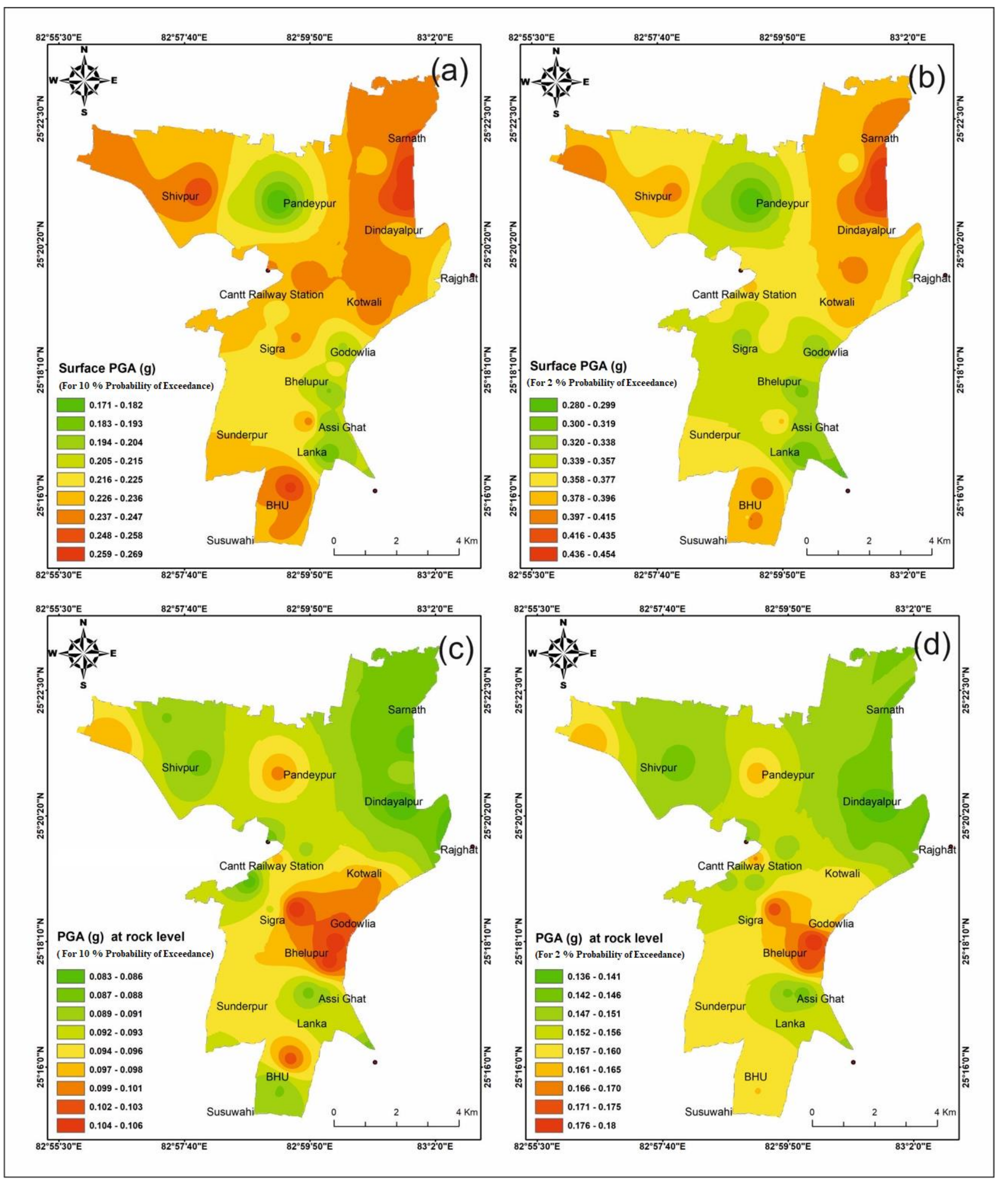

Figure 6. Spatial plots of expected PGA values. **(a)** Surface level for 10 % probability of exceedance in 50 years, **(b)** Surface level for 2 % probability of exceedance in 50 years, **(c)** Rock level for 10 % probability of exceedance in 50 years, **(d)** Rock level for 2 % probability of exceedance in 50 years.

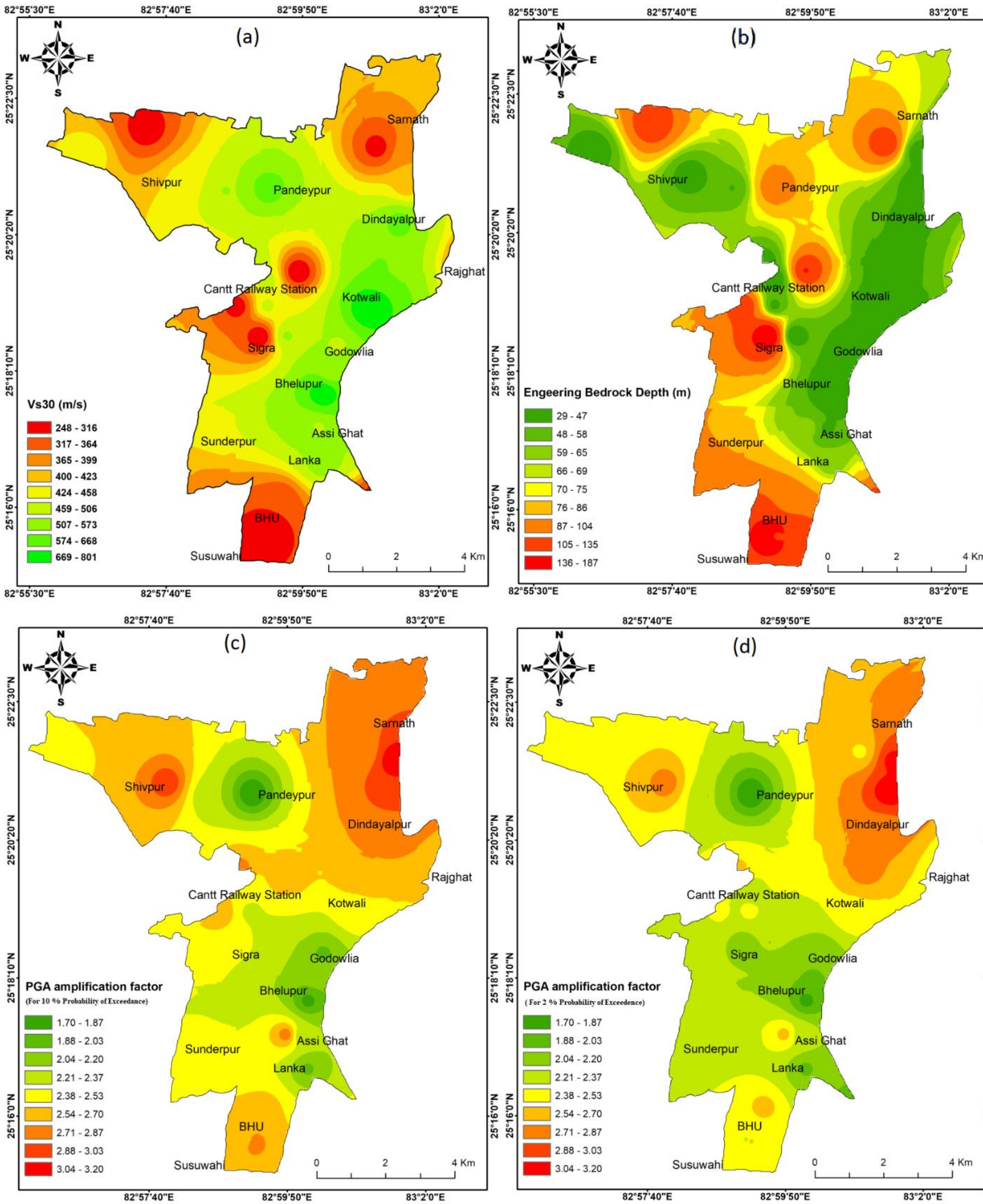

Figure 7. Results including the spatial plots of **(a)** Vs30, **(b)** engineering bedrock, **(c, d)** PGA amplification factor for 10% and 2% probability of exceedance in 50 years.

Sediment thickness and V_s30

The linear and polynomial best fit extrapolation technique was used to obtain the engineering bedrock depth, which varies from 29 to more than 150 m for the study region (Table 2). Soils above the water table are generally unsaturated, while those below are saturated, resulting in lower Vs values for saturated layers (Kramer, 1996). Water table depth used to validate Vs values depth wise. Water table depth data from Ground water brochure of Varanasi District, U.P. (Gautam, 2012) were used to validate the interpreted saturation profile and reconciled any discrepancies in the site response model (Idriss and Boulanger, 2008). Figure 7b shows that the engineering bedrock depth decreases as we move from SW to SE in Varanasi region. A higher thickness of sediment was observed to reach a velocity of 760 m/s in the BHU, Sigra, and Sarnath regions of the VDA, and a lower thickness was observed in the in the Godaulia, Kotwali, and Dindayalpur regions. As the shear wave velocity plays a crucial role in assessing the dynamic characteristic of the top sediment layers (Wald and Mori, 2000), site characterization and seismic hazard assessment often rely on determining the shear wave velocity near the surface. The Vs30 parameter is used to quantify the average shear wave velocity in the upper 30 meters of soil. It provides useful inputs for conducting in-depth study and gaining insight into the seismic characteristics of the underlying layers of the Earth's surface. The Vs30 values in Varanasi city range from 224 m/s to 801 m/s. Notably, Bhelupur and Kotwali regions exhibit higher Vs30 values, indicating stiffer soil conditions, which typically offer better seismic resistance. Conversely, areas such as BHU and Rajghat exhibit lower Vs30 values, suggesting softer soil that could amplify seismic waves (Garala and Madabhusi, 2019). The localities of Pandeypur, Sunderpur, and Cantt regions exhibit moderate Vs30 values, indicating intermediate soil conditions with a moderate seismic response.

Seismic Risk

Throughout the twentieth century, an average of approximately 17,000 individuals per year lost their lives due to building damage during earthquakes (Scawthorn and Chen, 2002). Notable earthquakes that have occurred in this region during last few decades include the 2005 Kashmir earthquake with a magnitude of 7.6, the 1991 Uttarkashi earthquake with a magnitude of 6.8, and the Bihar Nepal border earthquakes in 1934 and 1950 with magnitudes of 8.4 and about 8.6, respectively. The Shillong Plateau, located south of Bhutan, experienced a powerful earthquake in 1897 with a magnitude of 8.2. The 2015 Gorkha earthquake of magnitude 7.8, which caused massive damage Nepal also had an effect on the Indo-Gangetic Plain.

It has been argued that the current seismic quiescence in the Himalaya region is a phase of strain accumulation that may lead to a catastrophic earthquake in different segments of Himalaya (Bilham, 2004). Estimates suggest that the death toll from such an event could surpass 100,000 individuals. This projection highlights the urgent need for improved seismic preparedness, resilient infrastructure, and effective risk mitigation strategies to mitigate the devastating consequences of earthquakes in the region.

The risk assessment for Varanasi reveals a multifaceted background of seismic vulnerability, characterized by dynamic interplays between geological, geotechnical, and socio-economic factors. Spatial distribution of the PGA values across the city identify certain areas as hotspots for intense ground shaking and heightened structural damage. The analysis of Vs30 values further highlights soil characteristics as a critical determinant of seismic hazards, with softer soils amplifying ground motions and increasing vulnerability. The population density of Varanasi city varies from 10,254 to 1,32,324 people per square km, which shows significant population density changes (1300%) ward-wise. The population density shows (Figure 2), Kotwali, Bhelupura, Sigra, and Sunderpur as the pockets of high population density. Population density emerges as a key factor, with higher densities in vulnerable areas exacerbating socio-economic risks and complicating disaster response efforts. Spectral acceleration analysis also shows how important frequency-dependent ground motion characteristics are for designing structures and making sure infrastructure is resilient. Some locations, such as Assi Ghat, Kotwali, Shivpur, and Cantt region exhibit high PGA amplification along with high density and poor building construction and therefore can be considered high-risk areas. Overall, the risk assessment underscores the urgent need for comprehensive disaster risk reduction strategies informed by interdisciplinary approaches and tailored to the unique challenges of Varanasi's seismic landscape.

Table 2. Location of the data sources and results

ID	Latitude	Longitude	PGA (s) DBE	PGA (s) MCE	PGA (r) DBE	PGA (r) MCE	Vs30 (m/s)	EBRD (m)	WTD (m)
B1	25.27900	83.00256	0.185	0.301	0.092	0.154	552.73	59.76	5
B2	25.28780	83.00142	0.195	0.332	0.090	0.143	496.74	43.67	7
B3	25.29684	83.00272	0.192	0.311	0.105	0.175	791.55	29.36	3
B4	25.30272	83.00466	0.218	0.356	0.105	0.180	510.48	33.88	8
B5	25.30929	83.00670	0.202	0.324	0.101	0.157	492.07	35.15	2
B6	25.31210	82.99314	0.238	0.373	0.106	0.173	513.90	30.39	6
B7	25.31997	82.98786	0.219	0.346	0.094	0.146	469.24	42.42	8
B8	25.32662	82.98787	0.233	0.384	0.097	0.166	479.12	30.43	12
B9	25.33139	82.98521	0.240	0.369	0.085	0.144	491.93	33.73	2
B10	25.35052	82.97682	0.208	0.330	0.093	0.147	506.67	46.64	13
B11	25.35382	82.96585	0.256	0.403	0.087	0.143	427.53	36.98	19
B12	25.36025	82.94090	0.246	0.409	0.098	0.163	439.38	37.20	25.5
B13	25.31935	83.01497	0.243	0.392	0.099	0.159	800.97	32.60	6.5
B14	25.33108	83.01780	0.247	0.403	0.090	0.145	576.30	35.48	15
B15	25.34209	83.02300	0.229	0.386	0.083	0.136	608.14	39.53	12
B16	25.35157	83.02454	0.266	0.454	0.090	0.144	404.67	36.58	16
B17	25.35967	83.02550	0.269	0.454	0.084	0.145	397.13	35.82	20
B18	25.26894	82.99164	0.261	0.407	0.102	0.160	323.20	92.36	12
B19	25.26031	82.98728	0.227	0.365	0.089	0.157	289.94	168.87	14
M1	25.26000	82.98800	0.247	0.423	0.087	0.162	260.51	120.59	-
M2	25.26800	83.01600	0.197	0.261	0.083	0.144	263.84	122.01	-
M3	25.35100	82.98800	0.171	0.281	0.099	0.163	617.80	100.28	-
M4	25.36200	83.01700	0.231	0.368	0.087	0.147	289.73	124.82	-
M5	25.33000	83.04400	0.181	0.250	0.076	0.132	222.56	100.00	-
M6	25.28800	82.99700	0.240	0.379	0.087	0.145	535.61	62.17	-
M7	25.36700	82.95600	0.230	0.366	0.088	0.147	276.55	123.08	-
M8	25.32900	82.99600	0.245	0.359	0.090	0.148	248.45	136.94	-
M9	25.31200	82.98600	0.224	0.326	0.093	0.153	252.88	187.19	-
M10	25.32000	82.98000	0.228	0.363	0.084	0.149	271.92	124.66	-

PGA (s)- Peak Ground Acceleration at surface; PGA (r)- Peak Ground Acceleration at bed rock; DBE– Design basis earthquake; MCE- Maximum considered earthquake; Vs30- Average shear wave velocity for top 30m; EBRD- Engineering bedrock depth; WTD- Water table depth.

CONCLUSIONS

The Indo-Gangetic Plain is one of the highest seismic risk areas in the world. Due to its proximity to one of the world's most seismically active faults, Himalayan Frontal Thrust, thick alluvium, high exposure from densely populated towns, and the heightened susceptibility of buildings to earthquake damage, the Indo-Gangetic Plain poses a significant seismic risk. In this study, we attempted to examine the role of soil thickness and characteristics in seismic amplification for Varanasi City. The Vs30 values calculated for Varanasi City vary from 224 m/s to 801 m/s. These values indicate the stiffness of the soil that controls the seismic wave velocity, and therefore, the Vs30 map provides a first-hand approximation of the seismic hazard potential of the area, which is a valuable input for future infrastructural and urban planning. The results show that the area's local geology can amplify the PGA by 1.7 to 3.2 times for DBE and MCE scenarios. This implies that the actual seismic hazard in the area is much higher than expected for Zone III. This study highlights that though seismic zonation provides firsthand information on the earthquake risk in larger areas, surface geology further refines the risk estimate and provides crucial information for constructing building codes and urban planning.

Acknowledgements

The primary field data for the analysis was collected from the website of the Varanasi Development Authority. The authors are thankful to the editor and two anonymous reviewers for their critical input.

Author Credit Statement

AT: Conceptualization, modelling, data collection, manuscript writing; NR: Conceptualization, geological and tectonic inputs, manuscript writing; GPS: Manuscript writing.

Data availability

Data can be made available at a reasonable request.

Compliance with Ethical Standards

The authors declare no conflict of interest and adhere to copyright norms.

References

Agarwal, K., Singh, I., Sharma, M. and Rajagopalan, G., 2002. Extensional tectonic activity in the cratonward parts (peripheral bulge) of the Ganga Plain foreland basin, India. Int. J. Earth Sci., 91, 897–905. https://doi.org/10.1007/s00531-002-0265-z.

Akkar, S., Sandıkkaya, M.A. and Bommer, J.J., 2014. Empirical ground-motion models for point- and extended-source crustal earthquake scenarios in Europe and the Middle East. Bull. Earthq. Eng., 12, 359–387. https://doi.org/10.1007/s10518-013-9461-4.

Ambraseys, N.N., 2000. Reappraisal of north-Indian earthquakes at the turn of the 20th century. Curr. Sci., 79(9), 1237-1250.

Anbazhagan, P. and Sitharam, T.G., 2009. Spatial variability of the depth of weathered and engineering bedrock using the Multichannel Analysis of Surface Wave Method. Pure Appl. Geophys., 166, 409–428. https://doi.org/10.1007/s00024-009-0450-0.

Bajaj, K. and Anbazhagan, P., 2019. Seismic site classification and correlation between VS and SPT-N for deep soil sites in the Indo-Gangetic Basin. J. Appl. Geophys., 163, 55-72.

Bajaj, K. and Anbazhagan, P., 2020. Site Amplification Factors and Acceleration Response Spectra for Shallow Bedrock Sites – Application to Southern India. J. Earthq. Eng., 26(4), 2103-2123. https://doi.org/10.1080/13632469.2020.1754308.

Bakker, H., 1996. Construction and reconstruction of sacred space in Varanasi. Numen, 43(1), 32–55.

Bhukosh-GSI. Geological Survey of India, n.d. Bhukosh. Retrieved from https://bhukosh.gsi.gov.in/Bhukosh/MapViewer.aspx.

Bilham, R., 2004. Earthquakes in India and the Himalaya: Tectonics, geodesy and history. Ann. Geophys.. 47. 10.4401/ag-3338.

Bilham, R., 2009. The seismic future of cities. Bull. Earthq. Eng., 7(4), 839-887. https://doi.org/10.1007/s10518-009-9147-0.

Bilham, R., 2019. Himalayan earthquakes: A review of historical seismicity and early 21st-century slip potential. Geol. Soc. London, Special Publ., 483(1), 423-482. DOI: 10.1144/SP483.16

BIS., 2002. Bureau of Indian Standards, IS 1893–2002 Indian Standard Criteria for Earthquake Resistant Design of Structures—Part 1: General Provisions and Buildings. New Delhi: Bureau of Indian Standards.

Bommer, J.J., Crowley, H. and Pinho, R., 2015. A risk-mitigation approach to the management of induced seismicity. J. Seismol., 19, 623–646. https://doi.org/10.1007/s10950-015-9478-z.

Boore, D.M., 2003. Prediction of ground motion using the stochastic method. Pure Appl. Geophys., 160, 635–676.

Borcherdt, R.D., 1970. Effects of local geology on ground motion near San Francisco Bay. Bull. Seism. Soc. Am., 60(1), 29-60.

Borcherdt, R.D., 1994. Estimates of site-dependent response spectra for design (methodology and justification). Earthq. Spectra, 10(4), 617-653.

Celebi, M., Prince, J., Dietel, C., Onate, M. and Chavez, G., 1987. The culprit in Mexico City: Amplification of motions. Earthq. Spectra, 3(2), 315-328. https://doi.org/10.1193/1.1585431.

Choi, Y. and Stewart, J.P., 2005. Nonlinear site amplification as a function of 30 m shear wave velocity. Earthq. Spectra, 21. 1-30. https://doi.org/10.1193/1.1856535.

Cornell, C.A., 1968. Engineering seismic risk analysis. Bull. Seism. Soc. Am., 58(5), 1583-1606.

Denolle, M.A., Miyake, H., Nakagawa, S., Hirata, N. and Beroza, G.C., 2014. Long-period seismic amplification in the Kanto basin from the ambient seismic field. Geophys. Res. Lett., 41(7), 2319–2325. https://doi.org/10.1002/2014GL059425.

Garala, T.K. and Madabhushi, G.S.P., 2019. Seismic behaviour of soft clay and its influence on the response of friction pile foundations. Bull. Earthq. Eng., 17, 1919–1939. https://doi.org/10.1007/s10518-018-0508-4.

Gautam, J.P., 2012. Ground water brochure of Varanasi District, U.P. (A.A.P.: 2012-13). https://www.cgwb.gov.in/old_website/District_Profile/UP/Varanasi.pdf

Hough, S.E. and Bilham, R., 2008. Site response of the Ganges basin inferred from re-evaluated macroseismic observations from the 1897 Shillong, 1905 Kangra, and 1934 Nepal earthquakes. J. Earth Syst. Sci., 117(S2), 773-782. https://doi.org/10.1007/s12040-008-0068-0.

Hunter, J.A., Benjumea, B., Harris, J.B., Miller, R.D., Pullan, S.E., Burns, R.A. and Good, R.L., 2002. Surface and downhole shear wave seismic methods for thick soil site investigations. Soil Dyn. Earthq. Eng., 22(9–12), 931-941. https://doi.org/10.1016/S0267-7261(02)00117-3.

Idriss, I. and Boulanger, R.W., 2008. Soil liquefaction during earthquakes. San Francisco: Earthquake Engineering Research Institute.

Jha, P. and Bajwa, S., 2023. Cultural tangibles and intangibles and disaster challenges: Narratives from Varanasi. In: Singh, A. (Ed.), International Handbook of Disaster Research. Springer, Singapore. https://doi.org/10.1007/978-981-19-8388-7_60

Kanli, A.I., Tildy, P., Prónay, Z., Pinar, A. and Hermann, L., 2006. V_s^{30} mapping and soil classification for seismic site effect evaluation in Dinar Region, SW Turkey. Geophys. J. Int., 165, 223-235.

Khattri, K.N., Rogers, A.M., Perkins, D.M. and Algermissen, S.T., 1984. A seismic hazard map of India and adjacent areas. Tectonophysics, 108(1-2), 93-134. https://doi.org/10.1016/0040-1951(84)90156-2

Kramer, S.L., 1996. Geotechnical earthquake engineering. Prentice Hall, Upper Saddle River, New Jersey.

Kuo, C.H., Wen, K.L., Hsieh, H.H., Lin, C.M., Chang, T.M. and Kuo, K.W., 2012. Site classification and Vs30 estimation of free-field TSMIP stations using the logging data of EGDT. Eng. Geol., 129, 68–75. https://doi.org/10.1016/j.enggeo.2012.01.013

Mohamed, A.M.E., Hafiez, H.E.A. and Taha, M.A., 2013. Estimating the near-surface site response to mitigate earthquake disasters at the October 6th city, Egypt, using HVSR and seismic techniques. NRIAG J. Astron. and Geophys., 2(1), 146-165.

Nath, S.K. and Thingbaijam, K.K.S., 2009. Seismic hazard assessment – a holistic microzonation approach. Nat. Hazards Earth Syst. Sci., 9, 1445–1459. https://doi.org/10.5194/nhess-9-1445-2009

Nath, S.K., 2017. Probabilistic seismic hazard atlas of 40 cities in India. Geoscience Division, Ministry of Earth Sciences, New Delhi.

Nath, S.K., Adhikari, M.D., Maiti, S.K. and Ghatak C., 2019. Earthquake hazard potential of Indo-Gangetic Foredeep: its seismotectonism, hazard, and damage modeling for the cities of Patna, Lucknow, and Varanasi. J. Seismology, 23, 725–769. https://doi.org/10.1007/s10950-019-09832-3

Panjamani, A., Katukuri, A.K., Moustafa, S.S.R. and Al-Arifi, N.S.N., 2018. Seismic site classification and amplification of shallow bedrock sites. PLOS One, 13(12), 0208226. https://doi.org/10.1371/journal.pone.0208226

Parihar, A. and Anbazhagan, P., 2020. Site response study and amplification factor for shallow bedrock sites. Indian Geotech. J., 50, 726–738. https://doi.org/10.1007/s40098-020-00410-w

Puri, N. and Jain, A., 2020. Estimation of local site effect on earthquake ground motions for sites in the state of Haryana, India. In: Babu, K., Rao, H., Amarnath, Y. (eds) Emerging Trends in Civil Engineering. Lecture Notes in Civil Engineering, 61. Springer, Singapore. https://doi.org/10.1007/978-981-15-1404-3_10

Raghucharana, M.C., Somala, S.N., Erteleva, O. and Rogozhin, E., 2021. Seismic risk assessment for Central Indo-Gangetic Plains, India. Iranian J. Earth Sci., 13 (2), 77-93.

Rana, R.P.S., 2018, January. Urbanisation in Varanasi and interfacing historic urban landscapes. In: Urbanisation in Indian history: Proceedings of the National Seminar on “Urbanization in Indian History. 5-6.

RITES Ltd., 2016. Detailed Project Report for Rail-Based Mass Transit System in Varanasi, Final Report prepared for Varanasi Development Authority.

Sahu, S. and Saha, D., 2014. Geomorphologic, stratigraphic, and sedimentologic evidence of tectonic activity in Sone-Ganga alluvial tract in Middle Ganga Plain, India. J. Earth Syst. Sci., 123, 1335–1347. https://doi.org/10.1007/s12040-014-0470-8

Scawthorn, C. and Chen, W.F. (Eds.), 2002. Earthquake engineering handbook. Boca Raton: CRC Press. https://doi.org/10.1201/9781420042443

Seeber, L. and Armbruster, J.G., 1981. Great detachment earthquakes along the Himalayan Arc and long-term forecasting. In: Earthquake Prediction: An Int. Review, Am. Geophys. Union (Maurice Ewing Series), 4, 259-277. https://doi.org/10.1029/ME004p0259

Shukla, U.K. and Raju, N.J., 2008. Migration of the Ganga river and its implication on hydro-geological potential of Varanasi area, U.P., India. J. Earth Syst. Sci., 117(4), 489-498. https://doi.org/10.1007/s12040-008-0045-6

Shukla, U.K., Srivastava, P. and Singh, I.B., 2012. Migration of the Ganga river and development of cliffs in the Varanasi region, India during the late Quaternary: role of active tectonics. Geomorphology, 171-172, 101-113. https://doi.org/10.1016/j.geomorph.2012.05.012

Singh, I.B., Ansari, A.A., Chandel, R.S. and Misra, A., 1996. Neotectonic control on drainage system in Gangetic Plain, Uttar Pradesh. J. Geol. Soc. India, 47, 599–609.

Singh, M., Duggal, S. and Singh, V., 2020. A study to establish regression correlation between shear wave velocity and "N"-Value for Varanasi city, India. Proc. National Acad. Sci., India, Section A Physical Sciences, 91, 1-7. https://doi.org/10.1007/s40010-020-00686-w

Singh, M., Prasad, A. and Bajpai, M., 2023. Futuristic study on seismic response analysis of North Indian soils– A sustainable approach. Sustainable Futures, 6, 100141. https://doi.org/10.1016/j.sftr.2023.100141

Stein, S. and Wysession, M., 2003. An introduction to seismology, earthquakes, and Earth structure. Malden, MA: Blackwell Publishing.

USGS, 2024. U.S. Geological Survey, Earthquake hazard program. Available at: https://www.usgs.gov/programs/earthquake-hazards/how-seismic-waves-affect-different-size-buildings.

VDA, 2022. Varanasi Development Authority, Official website. Available at: https://vdavns.com

Wald, L.A. and Mori, J., 2000. Evaluation of methods for estimating linear site-response amplifications in the Los Angeles region. Bull. Seism. Soc. Am., 90(6B), S32–S42.

Yoshida, N. and Suetomi, I., 1996. DYNEQ: a computer program for dynamic analysis of level ground based on equivalent linear method. Reports of Engineering Research Institute, Sato Kogyo Co., Ltd., 61-70.

Received on: 19-06-2024 ; Revised on: 11-10-2024; Accepted on: 21-10-2024